ELSEVIER

www.elsevier.nl/locate/ica

Inorganica Chimica Acta 309 (2000) 82–90

Inorganica Chimica Acta

Cu(II)-containing cross-linked polymers for the hydrolysis of 4-nitrophenyl phosphate

Q. Lu [a,b], Alok Singh [a], Jeffrey R. Deschamps [c], E.L. Chang [a,*]

[a] *Naval Research Laboratory, Code 6930, Washington, DC 20375-5348, USA*
[b] *Geo Centers, Inc., 10903 Indian Head Hwy., Ft. Washington, Washington, DC 20375, USA*
[c] *Naval Research Laboratory, Code 6030, Washington, DC 20375-5348, USA*

Received 17 March 2000; accepted 16 July 2000

Abstract

The protonation constants of *N*-(4-vinyl)benzyl ethylenediamine (**L1**), 1-(4-vinyl)benzyl diethylenetriamine (**L2**), 4-(4-vinyl)benzyl diethylenetriamine (**L3**), and the stability constants of their Cu(II) and Zn(II) complexes have been potentiometrically determined. The crystal structures of $[Cu(\mathbf{L1})_2][ClO_4]_2$ and $[Cu\mathbf{L2}(NO_3)_2]\cdot CH_3CO_2C_2H_5$ are reported. $[Cu(\mathbf{L1})_2][ClO_4]_2$ crystallizes in the monoclinic system with space group $P2_1/c$, having lattice parameters $a = 12.48(2)$, $b = 12.062(16)$, $c = 9.188(15)$ Å, $\beta = 97.46(7)°$, and $Z = 2$. $[Cu\mathbf{L2}(NO_3)_2]\cdot CH_3CO_2C_2H_5$ crystallizes in the monoclinic system with space group $P2_1/n$, having lattice parameters $a = 10.239(2)$, $b = 9.177(1)$, $c = 24.096(4)$ Å, $\beta = 95.99(1)°$, and $Z = 2$. Kinetic studies show that the Cu(II)-containing cross-linked polymers made from incorporating $[Cu(\mathbf{L1})_2]X_2$ and $[Cu\mathbf{L3}]X_2$ ($X = ClO_4^-$, NO_3^-) catalyze the hydrolysis of 4-nitrophenyl phosphate with first-order rate constants 1.33×10^{-5} and 1.04×10^{-6} s^{-1}, respectively, at 55°C and pH 8.5. © 2000 Elsevier Science B.V. All rights reserved.

Keywords: *N*-Alkylation; Crystal structures; Stability constants; Cross-linked polymers; Catalytic hydrolysis

---

1. Introduction

There has been extensive interest in the catalytic hydrolysis of phosphate esters because of its relevance to the breakdown of nucleic acids and potent organophosphate pesticides. Many low molecular weight metal complexes have been designed and synthesized to promote the hydrolysis of phosphate esters, and some of these model complexes provide enormous rate acceleration for the hydrolysis reactions [1–8].

While homogenous catalysis is efficient, it suffers from difficulty in separation of products from reactants/catalysts. This shortcoming, however, can be overcome by immobilizing the model compounds into a polymeric matrix [9–11]. An often-overlooked additional advantage of incorporating the monomeric metal complexes into a polymeric matrix is that the polymeric structure may confer catalytic reactivity to the otherwise non-reactive metal complexes. We report here the synthesis and stability constants of the Cu(II) and Zn(II) complexes formed by the polymerizable ligands **L1**–**L3** (Scheme 1) and the catalytic hydrolysis of 4-nitrophenyl phosphate by the Cu(II)-containing cross-linked polymers. These polymers are made by incorporating Cu(II) complexes of **L1**–**L3** into a trimethylolpropane trimethacrylate (trim) matrix. The crystal structures of $[Cu(\mathbf{L1})_2][ClO_4]_2$ and $[Cu\mathbf{L2}(NO_3)_2]\cdot CH_3CO_2C_2H_5$ are also described.

2. Experimental

2.1. Materials

$CuCl_2\cdot 2H_2O$, KCl, trim, and CO_2-free Dilut-it ampoules of KOH were obtained from Sigma Chemical Co., Fisher Scientific Co., TCI, and J.T. Baler Inc., respectively. All other chemicals including ethylenediamine, diethylenetriamine, 4-vinylbenzyl chloride, and 4-nitrophenyl phosphate were purchased from Aldrich Chemical Co.

---

[*] Corresponding author.

0020-1693/00/$ - see front matter
PII: S0020-1693(00)00241-3

2.2. Synthesis

2.2.1. N-(4-Vinyl)benzyl ethylenediamine (**L1**)

A solution of 4-vinylbenzyl chloride (1.52 g, 10 mmol) in dichloromethane (100 ml) was added dropwise to a stirred solution of ethylenediamine (2.4 g, 40 mmol) in dichloromethane (200 ml). The resulting mixture was stirred at room temperature (r.t.) for 4 h. The solvent was then removed on a rotary evaporator. The residue was purified by chromatography on silica gel (9/1 MeOH–NH_4OH) to give *N*-(4-vinyl)benzyl ethylenediamine as a brown oil (0.88 g, 50%). ^{1}H NMR of *N*-(4-vinyl)benzyl ethylenediamine dihydrochloride (D_2O), δ (ppm): 3.32 (m, 2H), 3.38 (m, 2H), 4.23 (s, 2H), 5.31 (d, 1H), 5.83 (d, 1H), 6.76 (q, 1H), 7.39 (d, 2H), 7.51 (d, 2H). ^{13}C NMR (D_2O), δ (ppm): 35.64, 43.78, 51.49, 116.19, 127.11, 129.52, 130.38, 136.00, 139.28.

2.2.2. 1-(4-Vinyl) benzyl diethylenetriamine (**L2**) and 4-(4-vinyl) benzyl ditheylenetriamine (**L3**)

A solution of 4-vinylbenzyl chloride (1.52 g, 10 mmol) in dichloromethane (100 ml) was added dropwise to a stirred solution of diethylenetriamine (4.12 g, 40 mmol) in dichloromethane (300 ml). The resulting mixture was stirred at r.t. for 4 h. Two mono-substituted isomers were separated by chromatography on silica gel (9/1 MeOH–NH_4OH). ^{1}H NMR of 1-(4-vinyl) benzyl diethylenetriamine trihydrochloride (D_2O), δ (ppm): 3.28 (m, 8H), 4.06 (s, 2H), 5.11 (d, 1H), 5.64 (d, 1H), 6.54 (q, 1H), 7.20 (d, 2H), 7.32 (d, 2H). ^{13}C NMR (D_2O), δ (ppm): 35.23, 42.08, 43.75, 44.75, 51.5, 115.41, 127.08, 129.21, 130.30, 135.83, 138.92. ^{1}H NMR of 4-(4-vinyl) benzyl diethylenetriamine trihydrochloride (D_2O), δ (ppm): 3.34 (m, 4H), 3.47 (m, 4H), 4.38 (s, 2H), 5.27 (d, 1H), 5.81 (d, 1H), 6.69 (q, 1H), 7.40 (d, 2H), 7.50 (d, 2H). ^{13}C NMR (D_2O), δ (ppm): 34.12, 49.68, 58.58, 116.44, 127.42, 127.77, 131.59, 135.89, 139.80.

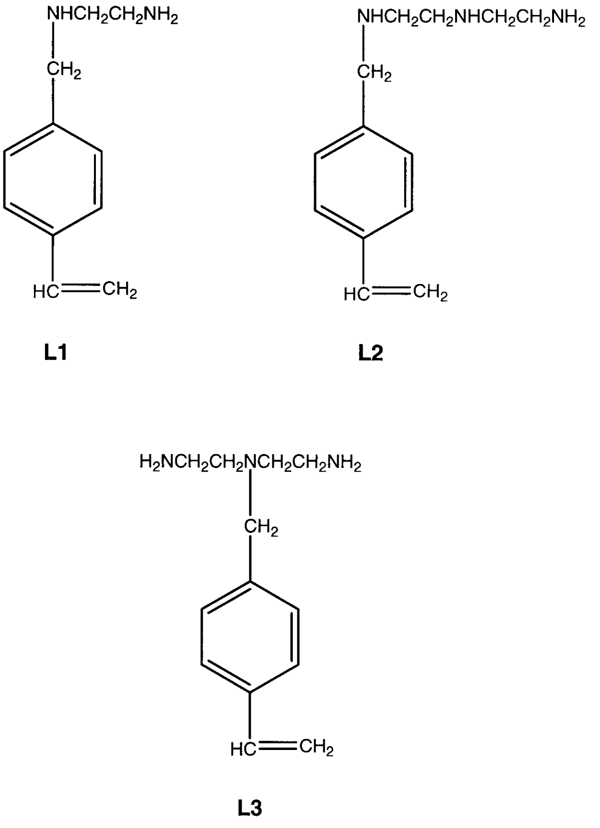

Scheme 1.

2.3. Preparation of crystalline Cu(II) complexes for X-ray analysis

2.3.1. [Cu(**L1**)$_2$][ClO_4]$_2$

N-(4-Vinyl)benzyl ethylenediamine (0.3 mmol) in methanol (10 ml) was mixed with a solution of $Cu(ClO_4)_2 \cdot 6H_2O$ (0.15 mmol) in acetonitrile (10 ml). Purple plate-like crystals suitable for X-ray analysis were collected after ether diffusion.

2.3.2. [Cu**L2**(NO_3)$_2$]·$CH_3CO_2C_2H_5$

1-(4-Vinyl)benzyl diethylenetriamine (0.15 mmol) in methanol (10 ml) was mixed with a solution of $Cu(ClO_4)_2 \cdot 6H_2O$ (0.15 mmol) in acetonitrile (10 ml). Ethyl acetate was diffused into the solution for several days, after which purple rod-like crystals suitable for X-ray analysis were collected.

2.4. Preparation of cross-linked polymers from Cu(II) complexes of **L1**–**L3** and trim

The following procedures were followed in the preparation of cross-linked polymers **Poly1**, **Poly2**, and **Poly3** from the Cu(II) complexes of **L1**–**L3** and trim. Substituted polyamine (1 mmol) was mixed with CuX_2 ($X = ClO_4^-$, NO_3^-) in a molar ratio of 1:1 or 2:1 in 25 ml EtOH. The mixture was stirred at r.t. for 15 min before trim (9 mmol in 10 ml EtOH) was added. The resulting solution was heated to 70°C while at the same time bubbling nitrogen. The initiator 2,2-azobisisobutyronitrile (AIBN) (100 mg) was then added to start the polymerization. Polymer formation could be seen within 1 h. Cross-linked polymers containing 10 mol% metal ion content to trim were isolated by filtration and washed with solvents to remove any unreacted starting materials.

Metal-free cross-linked polymers made from **L1**–**L3** and trim were also synthesized by the same procedures except without adding the Cu(II) salt.

Table 1
Crystal data and structure refinement parameters

Name	$[Cu(\mathbf{L1})_2][ClO_4]_2$	$[Cu\mathbf{L2}(NO_3)_2]\cdot CH_3CO_2C_2H_5$
Color/shape	purple/plate	purple/rod
Empirical formula	$C_{22}H_{32}Cl_2CuN_4O_8$	$C_{17}H_{29}CuN_5O_8$
Formula weight	614.96	494.99
Temperature	223(2) K	198(2) K
Crystal system	monoclinic	monoclinic
Space group	$P2_1/c$	$P2_1/n$
Unit cell dimensions		
a (Å)	12.48(2)	10.239(2)
b (Å)	12.062(16)	9.177(1)
c (Å)	9.188(15)	24.096(4)
β (°)	97.46(7)	95.99(1)
V (Å^3)	1372(4)	2251.8(6)
Z	2	4
D_{calc} (g cm^{-3})	1.489	1.460
Absorption coefficient (mm^{-1})	1.042	1.832
Diffractometer/scan	Bruker P4/θ/2θ	Bruker 1K CCD/ω
Radiation/wavelength (Å)	Mo Kα/0.71073	Cu Kα/1.54178
F(000)	638	1036
Crystal size	$0.22\times0.20\times0.08$ mm	$0.15\times0.11\times0.04$ mm
θ Range for data collection	2.36–25.08°	3.69–56.54°
Index ranges	$-14\leq h\leq 14$, $-14\leq k\leq 3$, $-2\leq l\leq 10$	$-8\leq h\leq 10$, $-9\leq k\leq 9$, $-26\leq l\leq 16$
Reflections collected	2684	7250
Independent/observed	2428/922	2600/2332
Absorption correction	face indexed	face indexed
Transmission factor range	0.88–0.98	0.76–0.92
Refinement method	full-matrix least-squares on F^2	full-matrix least-squares on F^2
Computing	XS [14], SHELXTL [15]	XS, [14] SHELXTL [15]
Data/restraints/ parameters	2428/13/273	2600/0/280
Goodness-of-fit (all data)	0.993	1.069
SHELXL weight parameters	0.0968 0.0000	0.0968 0.0000
R indices [$I>2\sigma(I)$]	$R_1=0.0808$ $wR_2=0.1791$	$R_1=0.0567$ $wR_2=0.1461$
R indices (all data)	$R_1=0.2179$ $wR_2=0.2576$	$R_1=0.0635$ $wR_2=0.1522$
Extinction coefficient	none	none
Largest difference peak and hole (e Å^{-3})	$0.310-0.284$	$0.626-0.595$

2.5. NMR and UV–Vis spectra

^{1}H and ^{13}C spectra were recorded on a Bruker AVANCE DRX 400 spectrometer. UV–Vis spectra were recorded on a Varian CARY 2400 spectrophotometer.

2.6. Crystallography

X-ray diffraction data for $[Cu(\mathbf{L1})_2][ClO_4]_2$ were collected on an automated four-circle diffractometer (Bruker P4) equipped with an incident beam graphite monochrometer and a 1.0-mm collimator. Three reflections, used as standards, were measured after every 97 new measurements. These standards showed a random variation of 2% over the period of data collection (approximately 24 h).

X-ray diffraction data for $[Cu\mathbf{L2}(NO_3)_2]\cdot CH_3CO_2C_2H_5$ were collected on a computer controlled Siemens CCD 1K area detector system with a Bruker platform goniometer, using a Rigaku rotating anode source and Göbels mirrors (Cu Kα radiation, $\lambda=1.54178$ Å). Data collection nominally covered a hemisphere in reciprocal space by combining six sets of exposures with different 2θ and φ angles: each exposure covered a range of 0.25° in φ. The crystal to detector distance was 4.48 cm and the coverage of a unique set was 94% complete to 1.0 Å resolution. Crystal decay was monitored by repeating 60 of the initial frames at the end of data collection. No crystal decay was found. The CCD data was integrated using SAINT [12]. Corrections were applied for Lorentz and polarization effects. A face-indexed absorption correction was applied using XPREP [13].

Data collection, structure solution, and refinement parameters for both crystal structures are summarized in Table 1. The structures were solved by direct methods with the program XS [14] and refined on F^2 using all reflections with the program SHELXTL [15]. Weighted R-factors (wR) and all goodness-of-fit parameters are based on F^2. Conventional R-factors (R) are based on F, with F set to zero for negative F^2.

For $[Cu(\mathbf{L1})_2][ClO_4]_2$, despite low temperature data collection, both the perchlorate and the 4-vinyl benzyl side chain were disordered. Secondary positions for the disorder were located in difference maps and refined using SHELXTL. Restraints were applied to the atoms in the perchlorate to preserve the geometry during the refinement of the disorder. The crystal scattered weakly with less than 40% of the data observed and R (σ) was 13.43%. Despite these problems the structure refined to a final R value of 8.08% for $I>2\sigma(I)$. The final R value of $[Cu\mathbf{L2}(NO_3)_2]\cdot CH_3CO_2C_2H_5$ is 5.67% for $I>2\sigma(I)$ (R (σ) for the data was 6.74% for the data).

2.7. Potentiometric measurements

Potentiometric studies of N-(4-vinyl)benzyl ethylenediamine dihydrochloride, 1-(4-vinyl)benzyl diethylenetriamine trihydrochloride, and 4-(4-vinyl)benzyl diethylenetriamine trihydrochloride in the absence and presence of metal ions were carried out with a Orion model 920A pH meter fitted with a Orion combined electrode. Each titration in aqueous solution was performed at 25.0°C and under nitrogen. The concentrations of the experimental solutions were approximately 2×10^{-3} to 4×10^{-3} M. The stoichiometries of ligand–metal ion systems are 1:1 and 2:1. Equilibrium constants were calculated with the program BEST [16]. The $\log K_w$ for the system, defined in terms of $\log [H^+][OH^-]$, was found to be -13.78 at the ionic strength employed and was fixed during the refinement of the other constants. In all the potentiometric determinations the σ_{fit} [16], which measures the deviation of the experimental curve and the curve calculated from the equilibrium constants, was less than 0.02[pH] units.

2.8. Kinetic studies

The method of initial rates was used to determine the rate constants of 4-nitrophenyl phosphate hydrolysis in the presence of **PolyL1**, **PolyL2**, and **PolyL3**. In a typical experimental run, 10 ml borate buffer (pH 8.5) containing substrate (in the range of 10^{-4}–10^{-3} M) was capped in a 15 ml test tube and placed in a thermostated bath (55 ± 0.5°C) equipped with a shaker. The reaction was initiated by adding 0.05 g Cu(II)-containing cross-linked polymer ($\sim 10^{-5}$ mol of Cu(II) ion). Periodically 0.2 ml of the solution was taken out by a syringe and diluted to 1 ml with borate buffer in a cuvette. The hydrolysis of 4-nitrophenyl phosphate was then followed through UV absorbance of 4-nitrophenylate at 400 nm. A reference solution was similarly prepared without the Cu-containing polymer in order to eliminate the effect from the spontaneous hydrolysis of 4-nitrophenyl phosphate. The initial rate of the reaction was obtained from the plot of 4-nitrophenyl phosphate concentration (calculated from the extinction coefficient of 4-nitrophenylate, 18700 l mol^{-1}) versus time. All the measurements were done in duplicate and the reactions were followed for less than 5% hydrolysis of the substrate. For the purpose of comparison, the kinetics of monomeric Cu(II) complexes of **L1**, **L2**, **L3** and the metal-free cross-linked polymers have also been also carried out under the same conditions.

3. Results and discussion

3.1. Crystal structure of $[Cu(\mathbf{L1})_2][ClO_4]_2$

The complex crystallizes in a monoclinic space group $P2_1/c$. The asymmetric unit contains one molecule of *N*-(4-vinyl)benzyl ethylenediamine, half a Cu(II) ion, and one perchlorate anion (Fig. 1). Bond lengths and angles are given in Tables 2 and 3. The coordination geometry around the Cu(II) ion is best described as square planar. One oxygen atom from each perchlorate anion is located above or below the plane at a distance of 2.553 Å. The bond length (2.05 Å) between the secondary nitrogen atom N2 and Cu(II) ion is slightly longer than that between the primary nitrogen atom N1 and the Cu(II) ion (1.974 Å), presumably due to the steric hindrance caused by the bulky substituent.

3.2. Crystal structure of $[Cu\mathbf{L2}(NO_3)_2]\cdot CH_3CO_2C_2H_5$

The complex crystallizes in a monoclinic space group $P2_1/n$. The asymmetric unit shown in Fig. 2 contains one molecule of 1-(4-vinyl)benzyl diethylenetriamine, one Cu(II) ion, one molecule of ethyl acetate, and two nitrate anions. Bond lengths and angles are listed in Tables 4 and 5. The Cu(II) ion is penta-coordinated by three nitrogen atoms from the tridentate polyamine and two oxygen atoms from the nitrate anions, exhibiting a square pyramidal geometry. The oxygen O1 from one of the nitrate anions occupies the apical position with a Cu–O1 distance of 2.314 Å. The bond length between the Cu(II) ion and the secondary nitrogen atom N7 is marginally longer than the other bond lengths between the Cu(II) ion and the nitrogen donors. The copper(II) cation is displaced 0.16 Å from the square planar basal plane.

3.3. The effect of *N*-alkylation on the basicity of **L1**, **L2**, **L3**, and the stability constants of their metal complexes

The protonation constants of **L1**, **L2**, **L3**, and the stability constants of their Cu(II) and Zn(II) complexes

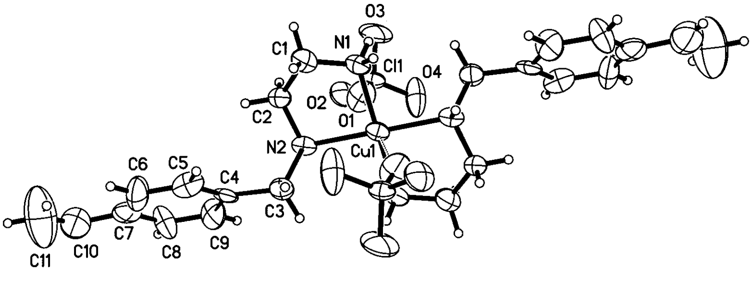

Fig. 1. View of $[Cu(\mathbf{L1})_2][ClO_4]_2$ showing the labeling of all non-hydrogen atoms. Thermal ellipsoids are shown at 20% probability level. H-atoms are drawn as small circles of arbitrary radii. Disordered positions of the divinylbenzene side-chain and perchlorate were omitted for clarity.

Table 2
Bond lengths (Å) for [Cu(**L1**)$_2$][ClO$_4$]$_2$

Atom 1	Atom 2	Distance	Atom 1	Atom 2	Distance
Cu1	N1	1.974(8)	C2′	N2′	1.55(5)
Cu1	N1[a]	1.974(8)	N2′	C3′	1.54(4)
Cu1	N2[a]	2.05(3)	C3′	C4′	1.56(3)
Cu1	N2	2.05(3)	C4′	C5′	1.3900
Cu1	N2′[a]	2.05(4)	C4′	C9′	1.3900
Cu1	N2′	2.05(4)	C5′	C6′	1.3900
N1	C1	1.433(18)	C6′	C7′	1.3900
C1	C2′	1.06(5)	C7′	C8′	1.3900
C1	C2	1.55(3)	C7′	C10	1.61(3)
C2	N2	1.46(3)	C8′	C9′	1.3900
N2	C3	1.44(2)	C10	C11	1.224(17)
C3	C4	1.57(2)	Cl1	O1	1.35(3)
C4	C5	1.3900	Cl1	O3	1.35(2)
C4	C9	1.3900	Cl1	O4	1.39(3)
C5	C6	1.3900	Cl1	O2	1.40(2)
C6	C7	1.3900	Cl1′	O3′	1.35(3)
C7	C8	1.3900	Cl1′	O1′	1.34(3)
C7	C10	1.50(3)	Cl1′	O2′	1.42(3)
C8	C9	1.3900	Cl1′	O4′	1.44(3)

[a] $-1-x$, $1/2+y$, $1/2-z$

Table 3
Bond angles (°) for [Cu(**L1**)$_2$][ClO$_4$]$_2$

Atom 1	Atom 2	Atom 3	Angle	Atom 1	Atom 2	Atom 3	Angle
N1	Cu1[a]	N1	180.0 (1)	C7	C8	C9	120.0
N1	Cu1[a]	N2	92.1(7)	C8	C9	C4	120.0
N1[a]	Cu1[a]	N2	87.9(7)	C1	C2′	N2′	124(3)
N1	Cu1	N2	87.9(7)	C2′	N2′	C3′	121(4)
N1[a]	Cu1	N2	92.1(7)	C2′	N2′	Cu1	101(2)
N2[a]	Cu1	N2	180.0 (1)	C3′	N2′	Cu1	108.1(18)
N1	Cu1[a]	N2′	98.5(10)	N2′	C3′	C4′	108(2)
N1[a]	Cu1[a]	N2′	81.5(10)	C5′	C4′	C9′	120.0
N2[a]	Cu1[a]	N2′	17.2(5)	C5′	C4′	C3′	128(2)
N2	Cu1[a]	N2′	162.8(5)	C9′	C4′	C3′	112(2)
N1	Cu1	N2′	81.5(10)	C4′	C5′	C6′	120.0
N1[a]	Cu1	N2′	98.5(10)	C5′	C6′	C7′	120.0
N2[a]	Cu1	N2′	162.8(5)	C8′	C7′	C6′	120.0
N2	Cu1	N2′	17.2(5)	C8′	C7′	C10	123(3)
N2′[a]	Cu1	N2′	180.0 (1)	C6′	C7′	C10	115(3)
C1	N1	Cu1	111.8(7)	C7′	C8′	C9′	120.0
C2′	C1	N1	115(3)	C8′	C9′	C4′	120.0
C2′	C1	C2	46(3)	C11	C10	C7	117(3)
N1	C1	C2	109.0(14)	C11	C10	C7′	116(3)
N2	C2	C1	115.3(18)	C7	C10	C7′	7.9(18)
C3	N2	C2	118.1(19)	O1	Cl1	O3	107.2(19)
C3	N2	Cu1	118.1(15)	O1	Cl1	O4	113(2)
C2	N2	Cu1	104.5(14)	O3	Cl1	O4	109(2)
N2	C3	C4	113.9(15)	O1	Cl1	O2	112(2)
C5	C4	C9	120.0	O3	Cl1	O2	110.5(19)
C5	C4	C3	119.2(16)	O4	Cl1	O2	104.8(19)
C9	C4	C3	120.7(16)	O3′	Cl1′	O1′	117(3)
C6	C5	C4	120.0	O3′	Cl1′	O2′	107.1(18)
C5	C6	C7	120.0	O1′	Cl1′	O2′	113.2(18)
C6	C7	C8	120.0	O3′	Cl1′	O4′	111.3(19)
C6	C7	C10	123(2)	O1′	Cl1’	O4′	103(2)
C8	C7	C10	117(2)	O2′	Cl1′	O4’	105(3)

[a] $-1-x$, $1/2+y$, $1/2-z$

have been determined by a potentiometric method. They are given in Tables 6 and 7 together with the corresponding constants of ethylenediamine (EN) and diethylenetriamine (DIEN) [17]. It is noted that *N*-alkylation reduces the basicity of **L1**, **L2**, **L3** and the stability constants of their complexes, in comparison with their parent polyamine ligands EN and DIEN. These observations seem to be in contradiction to what would be expected, as the 4-vinyl benzyl substituent is an electron-donating group. However, there are factors other than electron density that may exert an opposing influence on the basicity of *N*-alkylated polyamine ligands and the stability of their metal complexes. These factors include the steric hindrance caused by the bulky substituent that may elongate the M–N bonds, and the disruption of the hydrogen bonding pattern in aqueous solution, which may destabilize the positively-charged species such as protonated ligands and their metal complexes.

Crystal structure results show that the M–N bonds involving the secondary nitrogen atoms attached to a bulky substituent are only marginally longer than those involving the primary nitrogen atoms. Therefore, the steric factor may not be the most significant factor in reducing the basicity of **L1**, **L2**, **L3**, and their respective metal stability constants. Instead, the destabilization of positively charged species in aqueous solution from the disruption of the hydrogen bond is probably more

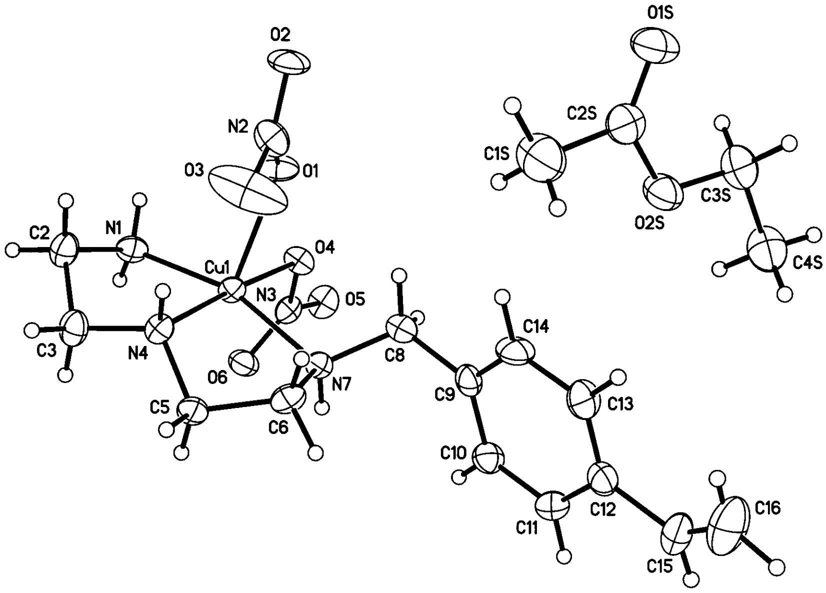

Fig. 2. View of $[CuL2(NO_3)_2]\cdot CH_3CO_2C_2H_5$ showing the labeling of all non-hydrogen atoms. Thermal ellipsoids are shown at 20% probability level. H-atoms are drawn as small circles of arbitrary radii.

Table 4
Bond lengths (Å) for $[CuL2(NO_3)_2]\cdot CH_3CO_2C_2H_5$

Atom 1	Atom 2	Distance	Atom 1	Atom 2	Distance
Cu1	N4	1.993(4)	Cu1	N1	1.996(4)
Cu1	O4	2.011(3)	Cu1	N7	2.038(4)
Cu1	O1	2.314(3)	N1	C2	1.482(6)
C2	C3	1.516(7)	C3	N4	1.461(6)
N4	C5	1.474(6)	C5	C6	1.520(7)
C6	N7	1.485(6)	N7	C8	1.485(6)
C8	C9	1.502(7)	C9	C14	1.384(7)
C9	C10	1.400(7)	C10	C11	1.376(7)
C11	C12	1.399(8)	C12	C13	1.369(8)
C12	C15	1.475(7)	C13	C14	1.389(7)
C15	C16	1.305(9)	N2	O2	1.228(6)
N2	O3	1.248(6)	N2	O1	1.256(5)
N3	O5	1.235(5)	N3	O6	1.241(5)
N3	O4	1.285(5)	C1S	C2S	1.497(8)
C2S	O1S	1.199(7)	C2S	O2S	1.337(7)
O2S	C3S	1.459(6)	C3S	C4S	1.515(8)

Table 5
Bond angles (°) for $[\mathrm{Cu}\mathbf{L2}(\mathrm{NO_3})_2]\cdot\mathrm{CH_3CO_2C_2H_5}$

Atom 1	Atom 2	Atom 3	Angle	Atom 1	Atom 2	Atom 3	Angle
N4	Cu1	N1	84.50(15)	N4	Cu1	O4	176.0(2)
N1	Cu1	O4	95.57(14)	N4	Cu1	N7	85.6(2)
N1	Cu1	N7	162.4(2)	O4	Cu1	N7	93.3(1)
N4	Cu1	O1	98.7(2)	N1	Cu1	O1	98.5(2)
O4	Cu1	O1	85.2(1)	N7	Cu1	O1	97.3(1)
C2	N1	Cu1	109.2(3)	N1	C2	C3	106.4(4)
N4	C3	C2	107.2(4)	C3	N4	C5	116.8(4)
C3	N4	Cu1	108.9(3)	C5	N4	Cu1	107.2(3)
N4	C5	C6	106.2(4)	N7	C6	C5	108.6(4)
C8	N7	C6	113.7(4)	C8	N7	Cu1	114.6(3)
C6	N7	Cu1	106.9(3)	N7	C8	C9	115.7(4)
C14	C9	C10	118.0(5)	C14	C9	C8	120.2(5)
C10	C9	C8	121.8(5)	C11	C10	C9	120.3(5)
C10	C11	C12	121.6(5)	C13	C12	C11	117.8(5)
C13	C12	C15	122.0(5)	C11	C12	C15	120.2(5)
C12	C13	C14	121.3(5)	C9	C14	C13	121.0(5)
C16	C15	C12	127.8(6)	O2	N2	O3	120.9(4)
O2	N2	O1	121.7(4)	O3	N2	O1	117.4(5)
N2	O1	Cu1	128.0(3)	O5	N3	O6	122.5(4)
O5	N3	O4	118.6(4)	O6	N3	O4	118.8(4)
N3	O4	Cu1	109.6(3)	O1S	C2S	O2S	123.8(5)
O1S	C2S	C1S	125.2(5)	O2S	C2S	C1S	111.0(5)
C2S	O2S	C3S	116.3(4)	O2S	C3S	C4S	107.3(5)

Table 6
Stepwise protonation constants of L ($\mu = 0.10$ M (KCl), 25.0°C, L = **L1**, **L2**, **L3**, EN, and DIEN, H = H^+) [a]

Equilibrium quotient	Log K				
	L1	**L2**	**L3**	EN	DIEN
[LH]/[L][H]	9.70(±2)	9.83(±2)	9.92(±4)	9.92(±5)	9.86(±7)
$[LH_2]/[LH][H]$	6.50(±1)	8.49(±2)	9.09(±3)	7.08(±4)	9.02(±6)
$[LH_3]/[LH_2][H]$		4.05(±3)	<2.0		4.25(±6)

[a] Standard deviations in parentheses.

Table 7
Stability constants [a] of L–Cu(II) and L–Zn(II) systems ($\mu = 0.10$ M (KCl), 25.0°C; L = **L1**, **L2**, **L3**, EN, and DIEN; H = H^+)

Equilibrium quotient	Log K				
	L1	**L2**	**L3**	EN	DIEN
[LCu]/[L][Cu]	8.99(±1)	14.92(±4)	14.12(±1)	10.50(±6)	15.9(±1)
$[L_2Cu]/[LCu][L]$	6.99(±1)			9.10(±2)	
[LZn]/[L][Zn]	4.30(±3)	8.06(±4)	8.20(±3)	5.7(±1)	8.82
$[L_2Zn]/[LZn][L]$	4.14(±3)			4.90(±1)	

[a] Standard deviations in parentheses.

important. The latter may also cause the increase in acidity of the metal ion as a Lewis acid in the *N*-alkylated complexes [18]. Indeed, *N*-alkylated 1,4,7-trisisopropyl-1,4,7-triazacyclononane–Cu(II)Cl_2 is a better catalyst for the anaerobic catalyzed hydrolysis of DNA than the parent compound, 1,4,7-triazacyclononane–Cu(II)Cl_2 [19].

3.4. Kinetics studies

The rates of 4-nitrophenyl phosphate hydrolysis in the presence of either Cu(II) complexes of **L1**–**L3** or Cu(II)-containing cross-linked polymers, **Poly1**–**Poly3**, and the metal-free cross-linked polymers have been measured by UV–Vis spectroscopy at 55°C and pH 8.5.

Since each measurement was carried out relative to a reference solution containing the same buffer and prepared under the same conditions as for the sample solution, the catalytic contribution, if any, from the hydroxide or buffer may be ignored.

Of all the kinetic measurements taken, only **Poly1** and **Poly3** show observable reactivity with approximate first-order rate constants of 1.33×10^{-5} (Fig. 3) and 1.04×10^{-6} s^{-1}, respectively (the k_{obs} of the uncatalyzed hydrolysis of 4-nitrophenyl phosphate at 55°C and pH 8.36 is 4.7×10^{-7} s^{-1} [7]). The reactions are catalytic as judged by the amount of 4-nitrophenylate produced under the conditions of a large excess of substrate. Because some absorption of the 4-nitrophenylate anion by the polymers was observed [20], the above rate constants are likely to be lower than the actual values. In either case, the adsorption did not appear to poison the catalytic centers within the polymers. All other complexes showed no measurable rate enhancement over the spontaneous hydrolysis of 4-nitrophenyl phosphate under the same conditions.

The inability of the monomeric Cu(II) complexes of **L1**–**L3** to catalyze the hydrolysis of 4-nitrophenyl phosphate is not surprising. As has been observed in previous studies [21], the catalytic reactivity of the Cu(II) ion for hydrolysis decreases with increasing stability constants of the complexes. All three Cu(II) complexes have relatively high stability constants, indicating that the Cu(II) ions in the complexes are poor Lewis acids that only react weakly with the substrate. What is interesting is that the Cu(II)-containing cross-linked polymers **Poly1** and **Poly3**, contrary to the monomers, do exhibit catalytic reactivity in the hydrolysis of 4-nitrophenyl phosphate.

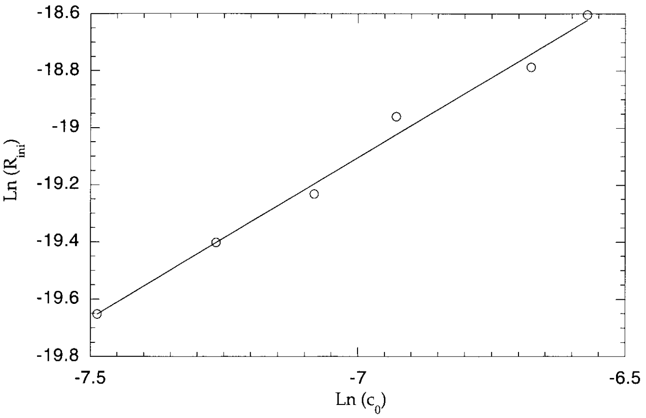

Fig. 3. The plot of the natural logarithms of the initial rates (R_{ini}) vs. the natural logarithms of the initial concentrations of 4-nitrophenyl phosphate for the system of **Poly1**–4-nitrophenyl phosphate (55°C, pH 8.5).

Table 8
Electronic spectra [a] of Cu(II) complexes of **L1**–**L3** and Cu-containing cross-linked polymers

Monomer	$[Cu(\mathbf{L1})_2][ClO_4]_2$	$[Cu\mathbf{L2}(NO_3)_2]$	$[Cu\mathbf{L3}(NO_3)_2]$
d–d transition (λ_{max}, nm)	540	650	667
Polymer	**Poly1**	**Poly2**	**Poly3**
d–d transition (λ_{max}, nm)	566	665	688

[a] In Nujol mull.

The electronic spectra (in Nujol mulls) of the Cu(II) complexes of **L1**–**L3** and the Cu(II)-containing cross-linked polymers **Poly1**–**Poly3** have been recorded. It is seen from Table 8 that there are slight red-shifts in the d–d transition bands of **Poly1**–**Poly3**, suggesting a possible distortion in the coordination geometry or the weakening of the Cu–N bonds in the polymer. These shifts in d–d transition bands, however, do not signify a major change either in the coordination geometry surrounding the Cu(II) ion or in the strength of the Cu–N bonds. Thus, the observed catalytic reactivity of **Poly1** and **Poly3** probably arises from the combined effect of the distortion of coordination geometry, the weakening of the Cu–N bonds, and the change in the general environment around the Cu(II) ion in the polymer matrix.

It is interesting to note that **Poly1** shows higher catalytic reactivity than **Poly3** even through one would expect the opposite by comparing the stability constants of $[Cu(\mathbf{L1})_2]^{2+}$ and $[Cu\mathbf{L3}]^{2+}$ ($10^{15.98}$ versus $10^{14.12}$). The better catalytic reactivity of **Poly1** may be due to its more porous structure since the monomer $[Cu(\mathbf{L1})_2]X_2$ contains one more polymerizable site than $[Cu\mathbf{L3}]X_2$. Obviously, a more porous structure will be beneficial for the substrate to gain access to the Cu(II) center.

Three conclusions may be drawn from the above results. First, the presence of the Cu(II) ion is a necessity for the observed catalytic reactivity since the metal-free cross-linked polymers show no activity. Second, the cross-linked polymer structure confers catalytic reactivity to the otherwise non-reactive Cu(II) centers, coordinated either by two molecules of **L1** or by one molecule of **L3**. Finally, the direct coordination of the Cu(II) ion to the substrate 4-nitrophenyl phosphate may be an important step in the cleavage of the P–O bond.

4. Supplementary material

Tables of anisotropic displacement parameters, H atom coordinates and isotropic displacement parameters for both crystal structures are available from the authors upon request. Crystallographic data for the structural analysis have been deposited with the Cambridge Crystallographic Data Center, CCDC 150132 and 150133 for compounds **L1** and **L2**, respectively. Copies of this information may be obtained free of charge from: The Director, CCDC, 12 Union Road, Cambridge, CB2 1EZ, UK (Fax: +44-1223-336033; e-mail: deposit@ccdc.cam.ac.uk or www: http://www.ccdc.cam.ac.uk).

Acknowledgements

The authors would like to acknowledge partial support of this work by the Office of Naval Research.

References

[1] N.H. Williams, W. Cheung, J. Chin, J. Am. Chem. Soc. 120 (1998) 8079.

[2] E.L. Hegg, S.H. Mortimore, C.L. Cheung, J.E. Huyett, D.R. Powell, J.N. Burstyn, Inorg. Chem. 38 (1999) 2961.

[3] R.A. Moss, K.G. Ragunathan, Langmuir 15 (1999) 107.

[4] P. Molenveld, S. Kapsabelis, J.F.J. Engbersen, D.N. Reinhoudt, J. Am. Chem. Soc. 119 (1997) 2948.

[5] T. Koike, M. Inoue, E. Kimura, M. Shiro, J. Am. Chem. Soc. 118 (1996) 3091.

[6] N.P. Sadler, C-C. Chuang, R.M. Milburn, Inorg. Chem. 34 (1995) 402.

[7] W.H. Chapman, R. Breslow, J. Am. Chem. Soc. 117 (1995) 5462.

[8] R.L. Fanshawe, A.G. Blackman, Inorg. Chem. 34 (1995) 421.

[9] N. Kim, J. Suh, J. Org. Chem. 59 (1994) 1561.

[10] P.S. Hammond, J.S. Forster, J. Appl. Poly. Sci. 43 (1991) 1925.

[11] F.M. Menger, T. Tsuno, J. Am. Chem. Soc. 111 (1989) 4903.

[12] Siemens (1995), SMART and SAINT, Data collection and processing software for the SMART system, Siemens Analytical X-ray Instruments Inc., Madison, WI, USA.

[13] XPREP, Version 5.10, Bruker Analytical X-ray Systems, 1997.

[14] XS, Version 5.10, Bruker Analytical X-ray Systems, 1997.

[15] SHELXTL, Version 5.10, Bruker Analytical X-ray Systems, 1997.

[16] A.E. Martell, R.J. Motekaitis, Determination and Use of Stability Constants, second ed., VCH, New York, 1992.

[17] A.E. Martell, R.M. Smith, R.J. Motekatis, NIST Critical Stability Constants of Metal Complexes Database 46, Version 3.0, NIST, Washington, DC, 1996.

[18] D. Meyerstein, Coord. Chem. Rev. 185–186 (1999) 141.

[19] E.L. Hegg, J.N. Burstyn, Inorg. Chem. 35 (1996) 7474.

[20] C. Hartshorn, A. Singh, E.L. Chang, in preparation.

[21] R.C. Courtney, R.L. Gustafson, S.J. Westerback, H. Hyytiainen, S.C. Chaberek, Jr., A.E. Martell, J. Am. Chem. Soc. 79 (1957) 3030.